Two-step Fabrication of Large Area SiO₂/Si Membranes

Viktoras GRIGALIŪNAS [1] [*], **Brigita ABAKEVIČIENĖ** [1], **Ignas GRYBAS** [2],
Angelė GUDONYTĖ [1], **Vitoldas KOPUSTINSKAS** [1], **Darius VIRŽONIS** [3],
Ramūnas NAUJOKAITIS [4], **Sigitas TAMULEVIČIUS** [1]

[1] *Institute of Materials Science of Kaunas University of Technology, Savanorių 271, LT-50131 Kaunas, Lithuania*

[2] *International Study Center, Kaunas University of Technology, Mickevičiaus 37, LT-44244 Kaunas, Lithuania*

[3] *Kaunas University of Technology, Panevėžys Institute, Daukanto 12, LT-35212 Panevėžys, Lithuania*

[4] *Kaunas University of Technology, Physics department, Studentų 50, LT-51368 Kaunas, Lithuania*

Two-step fabrication technique of SiO₂/Si membrane combining the deep local etching of double side polished and thermally oxidized silicon <100> wafer in tetramethylammonium hydroxide (TMAH) water solution and SF₆/O₂ reactive ion etching is presented in this study. The influence of temperature on stress and deformations of membrane was simulated using Solid Works software. The study of influence of photomask opening size on etching rate shows that TMAH etching rate $V = 0.44$ μm/min is higher for the biggest opening, whereas for smaller openings the etching rate is evidently decreased. It was revealed that TMAH during long etching time smoothly affects thermally grown silicon dioxide film as surface roughness R_a increases from 0.558 μm to 0.604 μm. SF₆/O₂ reactive etching rate is smoothly dependent on deep opening size when plasma power density varies from 0.25 W/cm² to 1.0 W/cm².

Keywords: SiO₂/Si membrane, TMAH etching, reactive ion etching, surface roughness.

1. INTRODUCTION

Large area free-standing membranes find applications in various microelectromechanical devices, e. g., pressure sensors, flow meters, thermopiles, microheaters etc. One of actual applications of free-standing membranes can be micro solid oxide fuel cells (μ-SOFC), where membrane is used as mechanical support to deposit active electrodes operating at the temperature up to 800 °C [1, 2]. Thermally grown silicon dioxide film seems to be very attractive for membrane's application due to the high etch selectivity over silicon in tetramethylammonium hydroxide (TMAH) or potassium hydroxide (KOH) solutions. On the other hand, fabrication of large area membrane is still a problem because many factors affect the fracture strength of bulk micromachined silicon dioxide membranes: besides key factors – membrane area and thickness, the fracture strength of the membrane is determined by the shape of the sidewalls and intersections, surface roughness, misorientation to the crystallographic axes [3], wafer material, point defects, membrane stress and microstructure [4–6]. Buckling effect of membranes caused by thermoelastic stresses can lead to membrane cracking [7]. Despite anisotropic etching of Si <100> in TMAH or KOH solution leaving free-standing silicon dioxide membrane is a well-known technique [8, 9], the final etching step of which is always critical, and large membranes often break due to the described reasons.

In this study TMAH is chosen as anisotropic etchant due to its low toxicity and absence of K⁺ contamination often encountered in KOH solution [10–12]. Moreover, TMAH almost does not attack silicon dioxide film

(compared to the KOH) in such a way being a more "protective" material [13–15].

In our research we propose two-step fabrication technique of reliable large area SiO₂/Si membrane, which can be used, e. g., as temporary support to deposit porous thin film electrodes for μ-SOFC. The first step of membrane fabrication is based on a deep local TMAH etching of a double side polished and thermally oxidized silicon wafer leaving just about a few per cent of unetched silicon beneath SiO₂ film. The second step of membrane fabrication acts as the final dry (and much more exact) SF₆/O₂ reactive ion etching [16] leading to just some microns of silicon left under SiO₂ membrane helping to prevent the structure from breakage. Subsequently supporting SiO₂/Si film, e. g., in case of μ-SOFC can be "lifted-off" using aqueous hydrofluoric acid solution. Since the dependence of etching parameters on membrane area is still not clearly defined in different works, we analyzed the effects of membrane area on stress and deformations by CAD simulation and carried out experimental tests revealing these relations.

2. EXPERIMENTAL TECHNIQUES

Both sides of double side polished single crystal Si <100> substrate (thickness – 500 μm) were thermally oxidized. Thickness of SiO₂ film (measured by a laser ellipsometer) was 1.08 μm. Patterning of wafers applying a photomask containing initial openings having different sizes (from 3×3 mm² to 0.5×0.5 mm² with step equal to 0.5 mm) was performed by standard optical lithography using ma-P 1225 photoresist (Micro Resist Technology GmbH). SiO₂ film was etched by NH₄F : HF : H₂O solution in the exposed areas. Wet etching of silicon (without agitation) was carried out using a 25 % TMAH solution (Sigma-Aldrich) heated up to 85 °C using a hot plate.

---
[*]Corresponding author. Tel.: + 370-670-19170; fax.: +370-37-314423.
E-mail address: *Viktoras.Grigaliunas@ktu.lt* (V. Grigaliūnas)

The second step was SF_6/O_2 reactive ion etching of remaining Si layer using PK-2420RIE (Plasma – Therm. Inc.) system. A constant flow mixture of sulphur hexafluoride and oxygen gas (10 sccm of SF_6 and 2 sccm of O_2) helped to generate plasma power which varied from 0.5 kW to 2.0 kW (plasma power density N varied from 0.25 W/cm^2 to 1.0 W/cm^2) with pressure in the chamber being 40 Pa. Bias voltage of cathode (U_b) varied from 200 V to 300 V. Temperature of the wafer was constant (20 °C).

Etched wafers were analysed using a high resolution scanning electron microscope FEI Quanta 200 FEG (accelerating voltage varried from 0.2 kV to 30 kV; resolution – 1.2 nm) and Raith e-LiNE scanning electron microscope mode.

Surface roughness of SiO_2 film was measured by atomic force microscope Nanosurf easyScan 2. All measurements were carried out in dynamic mode (scanning resolution – 256×256, probe vibration frequency – 166 kHz, probe vibration amplitude – 0.2 V).

3. MODELLING OF THERMOELASTIC STRESSES AND DEFORMATIONS

Geometric modelling of SiO_2 membrane was executed employing Solid Works software (2011 version) with static computational model being developed using Simulation mode. Three different models of large membrane were generated. Namely, the square shape mask opening boundaries were: 3.0×3.0, 2.5×2.5 and 2.0×2.0 mm^2 leading to corresponding membrane areas of 1.58×1.58, 1.09×1.09 and 0.58×0.58 mm^2 (due to the etching angle of 54.74°). Thickness of a single-crystal silicon wafer was 500 μm, and that of silicon dioxide – 1 μm. Each of the "specimens" was constrained by reduction of the same degrees of freedom, what lead to imitation of natural behavior of membrane under ordinary environmental conditions. All models were developed to predict behaviour of large membranes at 20 °C, as compressive stresses of SiO_2 film arise when cooling SiO_2/Si substrate from thermal oxidation to the ambient temperature. Elastic limit of similar area and thickness membranes varies in the range of 300 MPa – 400 MPa [17, 18].

Fig. 1 represents temperature induced stress distribution of 1.58×1.58 mm^2 SiO_2 membrane with respect to generated model having membrane area of 1.58×1.58 mm^2. The maximal stress is concentrated in the centre of membrane. Relationship between the membrane area and corresponding values of stresses and deformations at 20 °C is revealed in Fig. 2 and Fig. 3. Increase in size of the membrane causes the rise in stress (especially at the membrane edges and corners). For instance, approximately 250 MPa is observed in case of 1.58×1.58 mm^2 membrane, while 223 MPa and 184 MPa are registered at the edges of membranes for appropriate smaller openings. Reduction of membrane area results in higher stress concentration in the centre of membrane, i. e. stress value of about 67 MPa is found in 0.58×0.58 mm^2 membrane comparing to roughly 51 MPa and 40 MPa in another two membranes.

Increase in deformation and change in membrane's shape is directly proportional to the enlargement of membrane area. For example, deformation of the largest membrane varies between 3.45 μm and 3.80 μm, while two smaller membranes are misshapened in the range of 1.81 μm – 2.30 μm and 1.38 μm – 1.82 μm, respectively when considering values at different locations of analyzed film. One should also note that when membrane is reduced significantly it becomes more corrugated being deformed not as uniformly as the neighbouring ones.
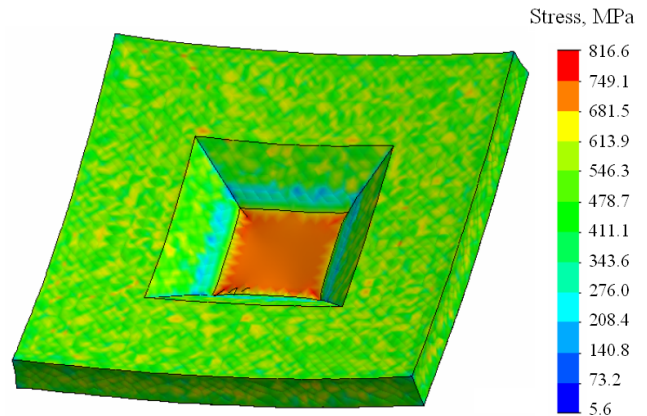

Fig. 1. Temperature induced stress distribution of 1.58×1.58 mm^2 SiO_2 membrane (in colour on-line)
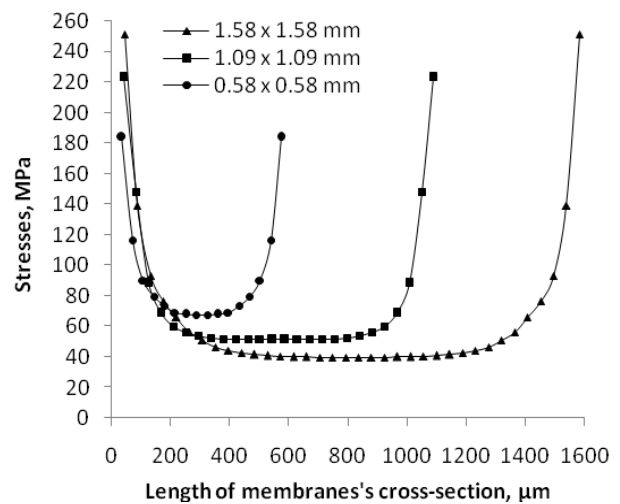

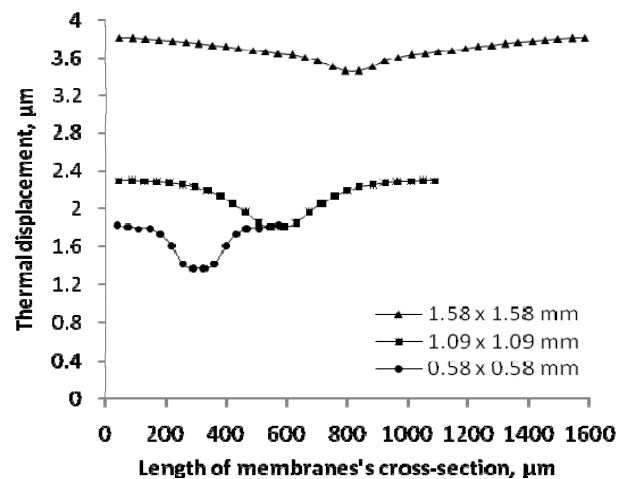**Fig. 2.** Temperature induced stress versus membrane area

Fig. 3. Temperature induced deformations versus membrane area

To sum up, it can be stated that the area is among the most critical parameters of membrane. Assumption can be made that difference in applied material properties (especially thermal expansion coefficient, Young's modulus, etc.) of silicon and silicon dioxide has a considerable impact on such results. As the stress values of large area membranes are close to the elastic limit and considering other factors conditioning the fracture strength of bulk micromachined SiO_2 membrane we can conclude that fracture limit can be surpassed leading to the cracks inside the membrane.

4. EXPERIMENTAL RESULTS AND DISCUSSION

TMAH, as anisotropic etchant, has a great deal of benefits comparing to other etchants. Due to its high selectivity with respect to SiO_2 mask a particularly even and smooth etched surface is obtained. It is particularly important that TMAH (as well as other anisotropic etchants) provides a unique form with respect to Si crystalline planes <100> and <111> (usually it is an angle of 54.74° between formed inclined slope and horizontal mask surface). High etching rate differences of appropriate crystallographic planes can be explained referring to individual distribution of atomic bonds and distinct density of atoms in those planes. Usually TMAH and other anisotropic mordants etch silicon significantly slower in <111> direction than in any other, and the etch ratio can even provide difference of order equal to 60 [13]. It is well defined that temperature and concentration of solution strongly influence the etching rate but impact of mask opening size on TMAH etching rate is still not well defined.

Table 1. TMAH etching parameters for different openings.

Opening size, mm^2	Distance A, μm	Etching depth H, μm	Etching time t, min	Etching rate V, μm/min
3×3	336	475	1080	0.440
2.5×2.5	318	450	1080	0.417
2×2	316	447	1080	0.414
1.5×1.5	316	447	1080	0.414
1×1	312	441	1080	0.408
0.5×0.5	302	427	1080	0.395

The etching parameters for different size openings were calculated from equal scale scanning electron microscope pictures by measuring the distance A (see Fig. 4), then obtaining the etching depth $H = (A/\sin(90° - 54.74°))^2 - A^2)$ and the etching rate $V = H/t$. The results are presented in Table 1.

It can be seen from Table 1 that although silicon <100> etching rate in 25 % TMAH solution at $T = 85\,°C$ is dependent on opening size but this dependence is not clearly expressed. Only for the biggest opening the etching rate $V = 0.44$ μm/min is evidently higher and approximately corresponds to the works of other authors [12, 13, 15], while for smaller openings the etching rate is decreased, though consequent dependence on opening size cannot be built relying on this experimental data. We just

can state that this dependence exists and it should be considered when etching small openings.

The influence of TMAH etching on surface roughness of SiO_2 film was evaluated using the atomic force microscope (Fig. 5). Average surface roughness R_a of unaffected specimen was 0.558 μm (root mean square roughness $R_q = 0.687$ μm). R_a of affected specimen was 0.604 μm ($R_q = 0.786$ μm). Basically there is a small difference in corresponding values of surface roughness characteristics what enables to state that TMAH etchant smoothly damages silicon dioxide layer during long etching time.
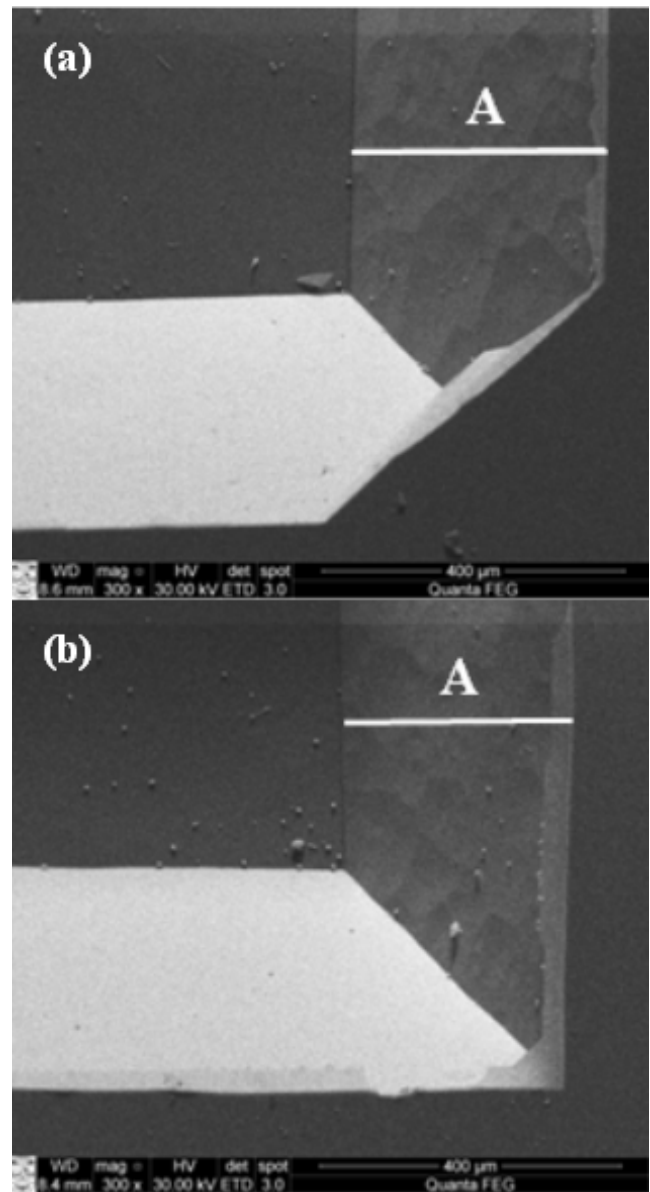

Fig. 4. Distance A for 3×3 mm (a) and 1×1 mm (b) openings

Because the final wet etching step is critical and experiments show that large membranes often break due to the high stresses at membrane edges and corners, a precise final SF_6/O_2 reactive ion etching was performed leading to just some microns of silicon left under SiO_2 membrane (Fig. 6). SF_6/O_2 reactive ion etching being not so dependent on crystal planes is well controlled process and ensures well-timed etching "stop" leaving undamaged SiO_2/Si membrane.
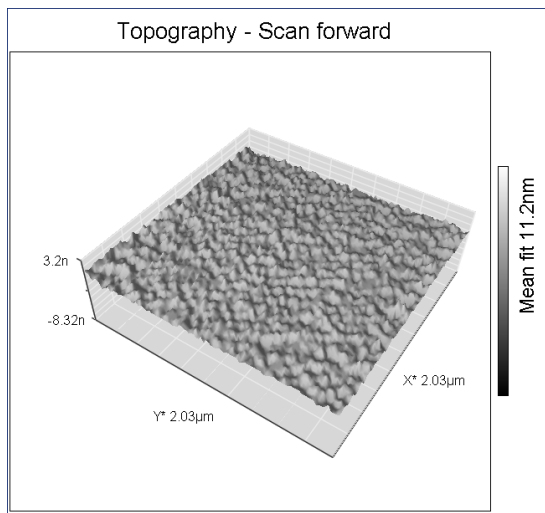
a
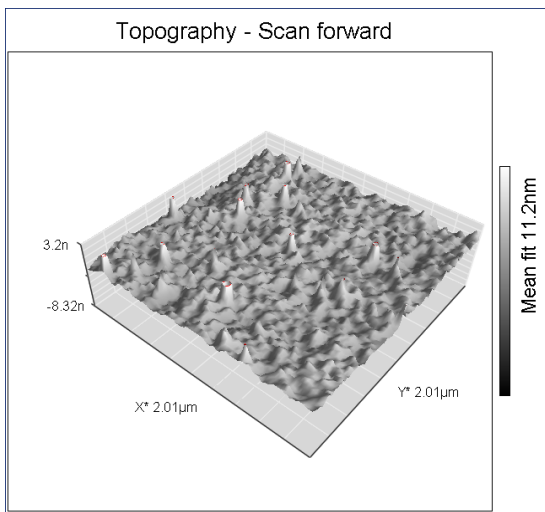
b

Fig. 5. Surface roughness of SiO_2 film before (a) and after (b) TMAH etching ($t = 1080$ min)
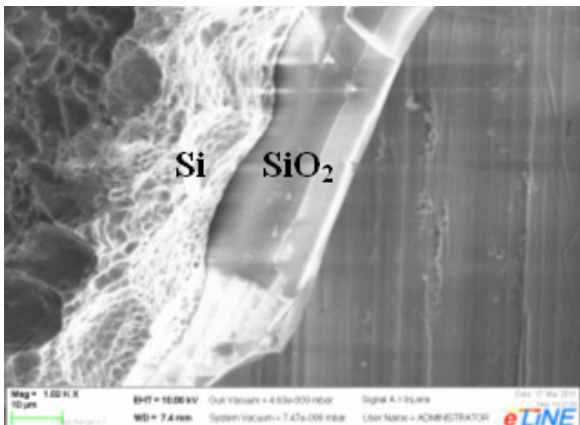

Fig. 6. Cross-section of SiO_2/Si membrane during final SF_6/O_2 reactive ion etching

Fig. 7 shows reactive ion etching rate of silicon (left after TMAH etching) versus SF_6/O_2 gas plasma power density and opening size (A – 3×3 mm^2, B – 0.5×0.5 mm^2). Generally addition of O_2 to SF_6 plasma leads to formation of F, O, SF_x radicals. Occuring O_2 and SF_x reaction increases concentration of F atoms assisting to generate the volatile compounds (SO, SOF, SO_2, SOF_4, etc.).
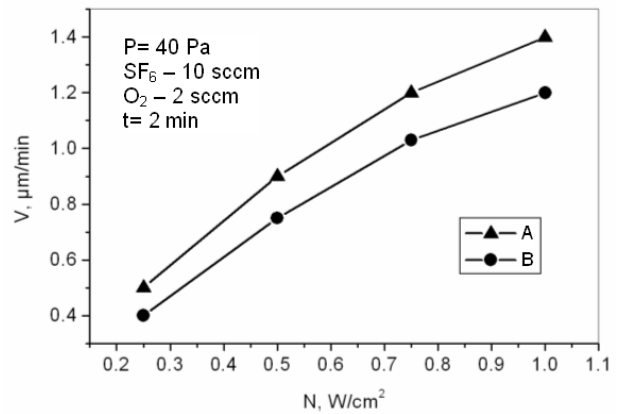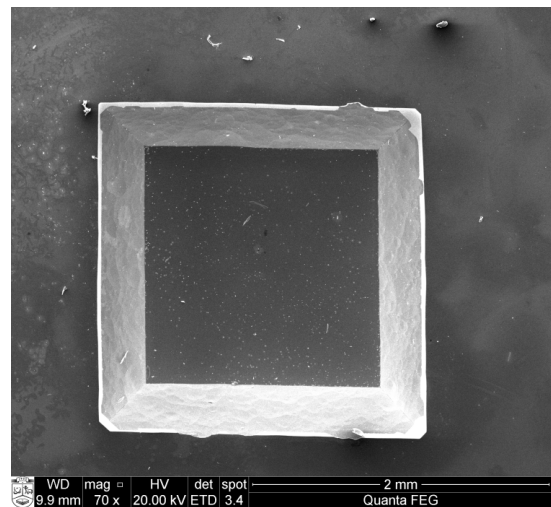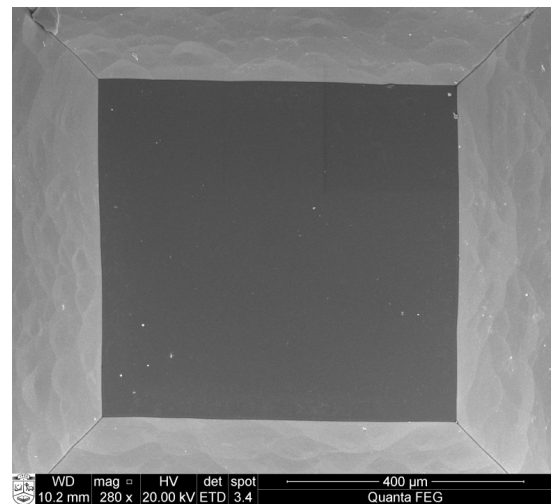

Fig. 7. Reactive ion etching rate versus SF_6/O_2 plasma power density for large and small opening (A – 3 mm × 3 mm, B – 0.5 mm × 0.5 mm)

a

b

Fig. 8. Two-step fabricated large (a, mark size 2 mm) and small (b, mark size 0.4 mm) SiO_2/Si membranes

Addition of O_2 increases the vertical etching rate of silicon due to enlarged F atoms concentration. On the contrary, growing passivating $Si_xO_yF_z$ film reduces rise of etching rate [11]. Extended etching time leads to the formation of sulphur polymers on the surface of silicon, and etching rate decreases. As we found, increase in plasma power density from 0.25 W/cm^2 to 1.0 W/cm^2 for

opening size of 3×3 mm^2 leads to the rise of etching rate from 0.5 µm/min to 1.4 µm/min, and increase in plasma power density from 0.25 W/cm^2 to 1.0 W/cm^2 for opening size of 0.5×0.5 mm^2 leads to the rise of etching rate from 0.4 µm/min to 1.2 µm/min. As etching rate is determined by both physical sputtering and chemical etching constituents (sputtering of silicon atoms by SF$_x$ ions dominates at a lower pressure, and increase of pressure brings the chemical etching component), a presumption can be made that in case of larger opening more F atoms assist for chemical etching.

Finally, fabricated large (a) and small (b) SiO$_2$/Si membranes are shown in Fig. 8. Since quantity of defects as well as edge/corner stresses increases with membrane area, it should be particularly assessed when designing practical devices.

5. CONCLUSIONS

Two-step fabrication of SiO$_2$/Si membrane using tetramethylammonium hydroxide (TMAH) water solution and SF$_6$/O$_2$ reactive ion etching was performed on double side polished and oxide patterned silicon <100> wafers varying opening size from 3×3 mm^2 to 0.5×0.5 mm^2 with step 0.5 mm. The highest TMAH etching rate $V = 0.44$ µm/min was found for the biggest opening whereas for smaller openings the etching rate is decreased. Thermally grown silicon dioxide mask is slightly affected by long TMAH etching, as SiO$_2$ film surface roughness R_a increases from 0.558 µm to 0.604 µm. Increase in plasma power density from 0.25 W/cm^2 to 1.0 W/cm^2 leads to the rise of etching rate from 0.5 µm/min to 1.4 µm/min for the biggest opening and to the rise from 0.4 µm/min to 1.2 µm/min for the smallest opening. CAD simulation reveals that increase in size of the membrane contributes to the rise of deformations as well as stresses at membrane edges and corners.

REFERENCES

1. **Srikar, V. T., Turner, Kevin T., Ie, Tze Yung Andrew, Spearing, S. Mark.** Structural Design Considerations for Micromachined Solid-oxide Fuel Cells *Journal of Power Sources* 125 2004: pp. 62 – 69.

2. **Hasran, U. A., Kamarudin, S. K., Daud, W. R. W., Majlis, B. Y., Mohamad, A. B., Kadhum, A. A. H.** A Simple Thermal Oxidation Technique and KOH Wet Etching Process for Fuel Cell Flow Field Fabrication, *International Journal of Hydrogen Energy* 36 (8) 2011: pp. 5136 – 5142.
http://dx.doi.org/10.1016/j.ijhydene.2011.01.043

3. **Wilson, C. J., Beck, P. A.** Fracture Testing of Bulk Silicon Microcantilever Beams Subjected to a Side Load *Journal of Microelectromechanical System*s 5 (3) 1996: pp. 142 – 150.

4. **Blom, M. T., Tas, N. R., Pandraud, G., Chmela, E., Gardeniers, J. G. E., Tijssen, R., Elwenspoek, M., van den Berg, A.** Failure Mechanisms of Pressurized Microchannels: Model and Experiments *Journal of Micro-electromechanical Systems* 10 (1) 2001: pp. 158 – 164.
http://dx.doi.org/10.1109/84.911105

5. **Mitsuhiro Shikida, Kenichi Nanbara, Tohru Koizumi, Hikaru Sasaki, Michiaki Odagaki, Kazuo Sato, Masaki Ando, Shinji Furuta, Kazuo Asaumi.** A Model Explaining Mask-corner Undercut Phenomena in Anisotropic Silicon Etching: a Saddle Point in the Etching-rate Diagram *Sensors and Actuators A: Physical* 97 – 98 2002: pp. 758 – 763.

6. **Rodica Iosub, Carmen Moldovan, Modreanu, M.** Silicon Membranes Fabrication by Wet Anisotropic Etching *Sensors and Actuators A: Physical* 99 2002: pp. 104 – 111.

7. **Malhaire, C., Didiergeorges, A., Bouchardy, M., Barbier, D.** Mechanical Characterization and Reliability Study of Bistable SiO$_2$/Si Membranes for Microfluidic Applications, *Sensors and Actuators A: Physical* 99 2002: pp. 216 – 219.
http://dx.doi.org/10.1016/S0924-4247(01)00891-3

8. **Biswas, K., Kal, S.** Etch Characteristics of KOH, TMAH and Dual Doped TMAH for Bulk Micromachining of Silicon *Microelectronics Journal* 37 (6) 2006: pp. 519 – 525.

9. **Tiggelaar, R. M., van Male, P., Berenschot, J. W., Gardeniers, J. G. E., Oosterbroek, R. E., de Croon, M. H. J. M., Schouten, J. C., van den Berg, A., Elwenspoek, M. C.** Fabrication of a High-temperature Microreactor with Integrated Heater and Sensor Patterns on an Ultrathin Silicon Membrane *Sensors and Actuators A: Physical* 119 2005: pp. 196 – 205.

10. **Yan, Guizhen, Chan, Philip C. H., Hsing, I-Ming, Sharma, Rajnish K., Sin, Johnny K. O., Wang, Yangyuan.** An Improved TMAH Si-etching Solution without Atacking Exposed Aluminum *Sensors and Actuators A: Phys.* 89 2001: pp. 135 – 141.

11. **Chollet, F., Liu, H.** A (Not so) Short Introduction to MEMS. MicroMachines Centre, School of MAE, Nanyang Technological University, Singapore, 2006: p. 56.

12. **Chen, Ping-Hei, Peng, Hsin-Yah, Hsieh, Chia-Ming, Chyu, Minking K.** The Characteristic Behavior of TMAH Water Solution for Anisotropic Etching on Both Silicon Substrate and SiO$_2$ Layer *Sensors and Actuators A: Physical* 93 (2) 2001: pp. 132 – 137.
http://dx.doi.org/10.1016/S0924-4247(01)00639-2

13. **Kazuo Sato, Mitsuhiro Shikida, Takashi Yamashiro, Kazuo Asaumi, Yasuroh Iriye, Masaharu Yamamoto.** Anisotropic Etching Rates of Single-crystal Silicon for TMAH Water Solution as a Function of Crystallographic Orientation *Sensors and Actuators A: Physical* 73 1999: pp. 131 – 137.

14. **Jae Sung You, Donghwan Kim, Joo Youl Huh, Ho Joon Park, James Jungho Pak, Choon Sik Kang.** Experiments on Anisotropic Etching of Si in TMAH *Solar Energy Materials and Solar Cells* 66 2001: pp. 37 – 44.
http://dx.doi.org/10.1016/S0927-0248(00)00156-2

15. **Mitsuhiro Shikida, Kazuo Sato, Kenji Tokoro, Daisuke Uchikawa.** Differences in Anisotropic Etching Properties of KOH and TMAH Solutions *Sensors and Actuators A: Phys.* 80 (2) 2000: pp. 179 – 188.

16. **Rangelow, Ivo W.** Dry Etching-based Silicon Micro-machining for MEMS *Vacuum* 62 2001: pp. 279 – 291.

17. **Malhaire, C., Le Berre, M., Febvre, D., Barbier, D., Pinard, P.** Effect of Clamping Conditions and Built-in Stresses on the Thermopneumatic Deflection of SiO$_2$/Si Membranes with Various Geometries *Sensors and Actuators A: Phys.* 4 1999: pp. 174 – 177.

18. **Resnik, D., Aljančič, U., Vrtačnik, D., Možek, M., Amon, S.** Mechanical Stress in Thin Film Microstructures on Silicon Substrate *Vacuum* 80 2005: pp. 236 – 240.